*Earth and Planetary Science Letters*, 109 (1992) 355–371
Elsevier Science Publishers B.V., Amsterdam



[MK]

# Interpretation of temperature measurements from the Kaiko-Nankai cruise: Modeling of fluid flow in clam colonies

Pierre Henry [a], Jean-Paul Foucher [b], Xavier Le Pichon [a], Myriam Sibuet [b], Kazuo Kobayashi [c], Pascal Tarits [d], Nicolas Chamot-Rooke [a], Toshio Furuta [c] and Peter Schultheiss [e]

[a] *Laboratoire de Géologie, E.N.S., 24 rue Lhomond, 75231 Paris Cedex 05, France*
[b] *IFREMER, Centre de Brest, BP 70, 29263 Plouzané, France*
[c] *Ocean Research Institute, University of Tokyo, Minamidai 1-15-1, Tokyo 164, Japan*
[d] *Laboratoire de Géomagnétisme et Paléomagnétisme, IPGP, 4 place Jussieu, 75252 Paris Cedex 05, France*
[e] *Schultheiss Geotek, Marley Lane, Haslemere, Surrey GU27 3RF, UK*

Received May 14, 1991; revision accepted December 16, 1991

ABSTRACT

During the Kaiko-Nankai detailed submersible survey, numerous measurements of the temperature gradient inside the sediment were performed on the deepest active zone of fluid venting, which is situated on the anticline related to the frontal thrust, using the Ifremer T-Naut temperature probe operated from the submersible *Nautile*. We thus obtained the temperature structure below different types of clam colonies associated with fluid venting. We used the finite element method to model the thermal structure and fluid flow pattern of these vents and to determine the velocity of upward fluid flow through the colonies. On a biological basis, four types of clam colonies are defined. Each biological type has distinctive thermal characteristics and corresponds to a particular fluid flow pattern. Darcian flow velocity in the most active type of colony (type A) is of the order of 100 m/a. The total amount of fluid flowing through colonies in the studied area is estimated to be 200 $m^3\ a^{-1}$ per metre width of subduction zone. Most of the flow is vented through type A colonies. This value is more than one order of magnitude too high to be compatible with the amount of water available from steady-state compaction of sediments in the whole wedge. Thermal arguments suggest that downwelling of seawater occurs around type A colonies and that seawater is then mixed with upcoming fluids at a depth of 1 or 2 metres. Furthermore, finite element modeling shows that a salinity difference of a few parts per mil between the upcoming fluids and seawater is sufficient to drive convection around the colonies. As water samples from a few vents indicate that the fluid source should actually be significantly less saline than seawater, we propose that the very high fluid flows measured are a consequence of the dilution of the fluid of deep origin with seawater by a factor of 5 to 10.

## 1. Introduction

Fluid seeps associated with chemosynthetic biological communities and carbonate concretions have been observed during submersible exploration of several accretionary wedges. Such vents were found first on the Oregon wedge [1], then on the Nankai wedge during the 1985 Kaiko cruise [2], on mud volcanoes situated seaward of the Barbados wedge [3], and on the southern part of this wedge [4]. Crude temperature measurements inside colonies in Tenryu Canyon on Nankai wedge indicated that upward fluid flow velocities are probably of the order of 100 m/a [5]. At Oregon venting sites direct flow measurements and indirect measurements from concentration of chemical tracers gave velocity values close to 100 m/a [6]. Fluid flow velocity in seeps below colonies can be determined from measurements of temperature at shallow depth within the sediment and the percentage of surface covered by biological communities can be estimated from submersible observations. Combining these two observations provides a lower bound to the water flux out of the toe of the accretionary wedge. The contributions of other types of vents, like carbon-

Correspondence to: Pierre Henry, Laboratoire de Géologie, E.N.S., 24 rue Lhomond, 75231 Paris Cedex, France.

ate chimneys, and of widespread venting through intergranular permeability have to be estimated using a different method.

Two different instruments, both built by Ifremer, have been used for shallow temperature measurements. One is a long-term observatory, the OT 6000. Its purpose is to monitor variations of fluid flow through time in a clam colony. This instrument was deployed during the cruise at a site where the rate of upward flow was too low to affect the temperature profile. The response of the sediment to variations of the seawater temperature was shown to be compatible with sediment conductivities in the usual range for subsurface sediment (of the order of 1 W $m^{-1}$ $K^{-1}$) [7]. Then the instrument was placed for a two-month period over an active vent. Although significant variations of fluid flow were recorded during this period, the vent showed no abrupt change in flow regime, and appeared to be fluctuating about a thermal steady state [7]. This makes it possible to estimate the fluid flow velocity from instantaneous temperature measurements, as in this study.

The other instrument, the T-Naut, is operated from the submersible and is used to make repetitive measurements in and outside seeps. Four types of colonies have been defined on a biological basis [8]. Each type appears to have a characteristic thermal signature. Finite element modeling is used to estimate fluid flow velocity for each type. These results combined with a statistical survey of the surface covered by clams [7] give a total fluid flux value which is too high to be compatible with the measured background thermal gradient, implying that fluids seeping in clam colonies are diluted with seawater at a ratio of about 5 to 10. This result has prompted us to investigate the possibility of free convection in and around the colonies.

## 2. T-Naut probe measurements

Temperature is measured with thermistors at depths of 19, 29 and 49 cm into the sediment. In order to check consistency, two probes are set at the 49 cm depth. The average temperature differ-

TABLE 1

List of physical parameters

| | | |
|---|---|---|
| $k$ | permeability | see figures 5 and 8 |
| $\mu$ | water viscosity | $10^{-3}$ Pa s |
| $g$ | gravity | 10 m $s^{-2}$ |
| $s$ | salinity | sea water: 35‰ |
| $\rho_w$ | fluid density | sea water: 1027 kg $m^{-3}$ at 0°C |
| $c_w$ | fluid heat capacity | 3990 J $kg^{-1}$ |
| $\rho_g$ | grain density | 2700 kg $m^{-3}$ |
| $c_g$ | grain heat capacity | 800 J $kg^{-1}$ |
| $\varphi$ | porosity | 60 to 70% |
| $\rho c$ | sediment volumetric heat capacity | |
| | $\rho c = \varphi(\rho c)_w + (1-\varphi)(\rho c)_g$ | 3.3 to 3.5 $10^6$ J $m^{-3}$ |
| $\kappa$ | sediment thermal diffusivity | measured, see [7] |
| | $2.4 \pm .6 \times 10^{-7} < \kappa < 3.1 \pm 0.75 \times 10^{-7}$ $m^2$ $s^{-1}$ | |
| $\Lambda$ | sediment conductivity | about 1 W $m^{-1}$ $K^{-1}$ |
| | $\Lambda = \kappa.\rho c$ | $0.7 < \Lambda < 1.25$ W $m^{-1}$ $K^{-1}$ |
| $D$ | thermal diffusivity for fluid advection | |
| | $D = \Lambda/\rho_w c_w$ | 2.5 $10^{-7}$ $m^2$ $s^{-1}$ = 7.88 $m^2$ $a^{-1}$ |
| $D_c$ | diffusivity of salt in water | about $10^{-9}$ $m^2$ $s^{-1}$ |
| $\beta$ | dispersivity | 10 cm |

ence between these two probes indicate that the relative precision of measurements is of the order of 2 mK. The absolute value of the temperature is of course not known with the same accuracy. An additional probe measures the temperature of seawater. A relative calibration is made before each station and, after penetration, thermistors are kept in the sediment for 10 minutes to allow relaxation of frictional heating. Equilibrium temperature is extrapolated assuming a $1/t$ decay.

### *2.1. Correction of bottom-water temperature variations*

Fluctuations in the bottom-water temperature perturbate the T-Naut measurements. For example, data collected at Site 2 at the 2000 m depth are impossible to use because temperature variations at the bottom water are of the order of 1°C. At Site 1, at the 3800 m depth, these variations are only about 10 mK and the data are usable. One can only hope to correct approximately the measurements from these fluctuations, as a temperature recording (from the OT 6000) is available only for dives 8 and 12 [7] and as water temperature also varies with the location (as observed during dive 12 and 21).

Consider the way cold or hot fronts modify the temperature inside the sediment at a site where there is no fluid advection.

$$\delta T(z,t) = \delta T_0 \operatorname{erfc}\left(\frac{z}{\sqrt{4\kappa t}}\right) \tag{1}$$

is the variation of temperature at time $t$ and depth $z$ if a sudden variation $\delta T_0$ in water temperature occurs at time $t = 0$. $\kappa$ is the thermal diffusivity of the sediment ($\kappa = \Lambda/\rho c$), and is taken to be equal to 9 $m^2\ a^{-1}$ (see Table 1 and [7]). Figure 1 shows the disturbance of the temperature profile due to such a sudden change in bottom-water temperature. Less than 6 hours later, temperatures measured by probes within the sediment (at 19, 29 and 49 cm) are still unaffected, resulting in an offset between the temperature profile which remains linear and the measured bottom-water temperature. This phenomenon most probably explains a 13 mK offset observed during dive 4 (see Fig. 1a). Four days later, the temperature profile is again linear, but the value of the gradient is still slightly different (see Fig. 1b). Dive 8 took place four days after dive 4, and Fig. 1a shows that the temperature within the first 50 cm of sediment had time to

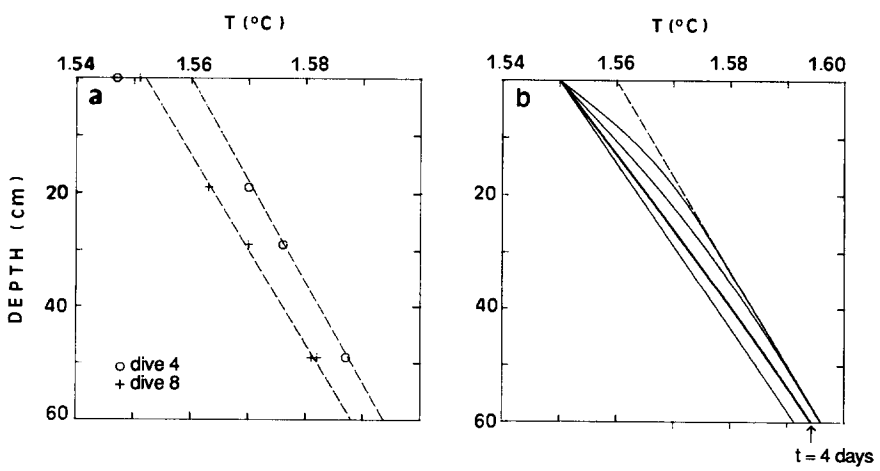


Fig. 1. Diffusion into the sediment of a sudden change of seawater temperature. a. *Reference measurements*. The shift between the conductive profile within the sediment and the seawater temperature observed during dive 4 disappeared by the time of dive 8, which took place 4 days later. b. *Diffusion model*. Theoretical relaxation of a 10 mK decrease in surface temperature at time $t = 4$ h, $t = 1$ day, $t = 4$ days and $t = 2$ weeks with thermal diffusivity $\kappa = 9\ m^2\ a^{-1}$ ($2.9 \times 10^{-6}\ m^2\ a^{-1}$). Temperature profile returns to linearity at $t = 4$ days.

TABLE 2

Gradient measurements

| Dive N°-Measure | Average gradient (mK/m) | Extrapolated surface T (°C) | Type of Profile | Distance to colony (m) | Comments |
|---|---|---|---|---|---|
| 4-1 | 59±1 | 1.558±0.000 | Linear | F | Reference |
| 2 | 56±0 | 1.560±0.000 | Linear | F | Reference, $T_{seawater}$=1.547°C |
| 3 | 61±1 | 1.563±0.001 | Linear | 0 | Type E colony |
| 4 | 62±1 | 1.560±0.000 | Linear | 0 | White patch & C colony |
| 5 | 90±4 | 1.567±0.002 | Linear | 0 | in a single E colony, |
| 6 | 105±7 | 1.566±0.003 | Sub-Lin | 0 | 50 cm apart |
| 7 | 83±2 | 1.562±0.001 | Linear | 1 | |
| 8 | 67±3 | 1.560±0.001 | Linear | 2 | |
| 9 | 73±4 | 1.565±0.002 | Linear | 0 | in 2 type E colonies, |
| 10 | 74±3 | 1.561±0.001 | Sub-Lin | 0 | 2 m apart |
| 12 | 52±4 | 1.587±0.001 | Linear | 0 | Type A colony |
| 13 | 76±3 | 1.559±0.001 | Linear | 2 | |
| 8-1 | 56±4 | 1.555±0.001 | Linear | 0.1 | |
| 2 | 30±3 | 1.575±0.001 | Sub-Lin | 0 | Type B colony |
| 3 | 57±4 | 1.559±0.002 | Linear | 0.5 | |
| 4 | 56±8 | 1.558±0.003 | Linear | 1 | 2 m from 8-6 |
| 5 | 65±7 | 1.555±0.003 | Sub-Lin | 1 | |
| 6 | 56±7 | 1.558±0.003 | Sub-Lin | 0 | Type E colony |
| 7 | 30±9 | 1.572±0.004 | Curved | 0 | Type B colony |
| 8 | 60±4 | 1.552±0.001 | Linear | F | Reference, $T_{seawater}$ =1.552°C |
| 9 | 75±8 | 1.551±0.002 | Sub-Lin | F | Reference |
| 10 | 71±14 | 1.559±0.005 | Odd | 0 | White patch & C colony |
| 12-1 | 23±20 | 1.608±0.008 | Curved | 0 | Type A colony |
| 2 | 21±11 | 1.609±0.004 | Curved | 0 | |
| 3 | 21±8 | 1.610±0.003 | Curved | 0 | |
| 4 | 37±2 | 1.559±0.001 | Linear | 1 | |
| 5 | 52±6 | 1.558±0.002 | Linear | 1 | $T_{seawater}$ = 1.549°C |
| 6 | 71±10 | 1.570±0.004 | 2 probes | 0 | Type A colony |
| 7 | 57±1 | 1.553±0.000 | Linear | 0.5 | |
| 8 | 84±3 | 1.555±0.001 | Linear | F | too far north |
| 9 | 69±3 | 1.552±0.001 | Linear | F | Reference, $T_{seawater}$ =1.549°C |
| 12 | 75±18 | 1.561±0.007 | Odd | F | near Puppi site 3 |
| 20-1 | 84±12 | 1.604±0.003 | Curved | 0 | Type A, $T_{seawater}$ = 1.560°C |
| 3 | 23±7 | 1.567±0.002 | Odd | 1.5 | both measurements |
| 4 | 19±7 | 1.572±0.003 | Odd | 1.5 | during one station |
| 21-1 | 53±7 | 1.558±0.003 | Sub-lin | F? | Reference for OT6000-2 |
| 2 | 49±3 | 1.592±0.001 | Sub-lin | 0 | Type A, $T_{seawater}$ = 1.556°C |

Underlined values are used as reference seafloor temperatures in thermal models

equilibrate with the new bottom-water temperature.

This argument leads us to consider that the mean seafloor temperature to be used in the computations can be estimated by extrapolating to the seafloor temperature profiles in the sediment which are not affected by fluid flow. When possible, a reference seafloor temperature is evaluated by this method. If this is not possible, we use the measured seawater temperature. Corresponding values are underlined in Table 2.

*2.2. First estimate of the upward velocity of fluid within clam colonies*

In order to obtain a first estimate of the upward water flow inside clam colonies, a one-dimensional steady-state model is used, assuming uniform advection of fluid in a uniform half-space (constant thermal diffusivity). The assumption that no heat is lost through the sides of the conduit which brings the fluid to the colony is implied. This is acceptable if temperature measurements are made to a depth that is small with respect to the diameter of the colony. As this is not the case (measurements are at the depths of 20, 30 and 50 cm whereas colonies are typically 50 cm to 2 m in diameter) the amount of fluid flowing through the colony is underestimated.

The steady-state temperature profile predicted using this one-dimensional model is exponential:

$$T(z) = T_0 + (T_\infty - T_0) \cdot \left[1 - \exp\left(-\frac{U_D z}{D}\right)\right] \quad (2)$$

where $U_D$ is the Darcy velocity and $D = \Lambda/(\rho c)_w$ is the thermal diffusivity relative to fluid flow. D is taken equal to $2.5 \times 10^{-7}$ m$^2$ s$^{-1}$ (see Table 1).

$T_0$ is the temperature at the surface of the sediment. $T_0$ actually varies with time. As already discussed, a reasonable correction of these variations can be made by taking $T_0$ equal to the reference temperature at the surface given in Table 2. This correction enables us to assume that the system was in thermal steady-state. However, estimates of $U_D$ from data depend significantly on the choice of $T_0$ when $U_D$ is small. Thus only Darcy velocities greater than 10 m/a can be reasonably estimated. The model has been applied only to colonies where a significant temperature increase was observed. Darcian flow velocity values obtained from a mean square best fit of the data by eq. (3) are given in Table 3.

TABLE 3

Darcian flow velocity inside the colonies with diffusivity $D = 2.5\ 10^{-7}$ m$^2$ s$^{-1}$

| Colony type | Dive | Measurement | $U_D$ (m/a) 1-D model | FEM | Conduit length (m) |
|---|---|---|---|---|---|
| A | 4 | 12 | * | 70 | 1.1 |
| A | 12 | 1,2,3 | 85 | 150 | 1.1 |
| A | 12 | 6 | 19 | * | * |
| A | 20 | 1 | 86 | 110 | 2 |
| A | 21 | 2 | * | 70 | 1.1 |
| B | 8 | 2 | 54 | 70 | 0.6 |
| B | 8 | 7 | 58 | 70 | 0.6 |
| C | 4 | 4 | - | - | |
| C | 8 | 10 | * | * | |
| E | 4 | 3 | - | - | |
| E | 4 | 5,6 | 9 | 30 | >10 |
| E | 4 | 9,10 | - | <15 | >2 |
| E | 8 | 6 | - | - | |

Hyphen indicates not enough flow to model by this method

* Unusable data

## 3. Classification of clam colonies

### 3.1. *Biological classification*

Several types of colonies have been defined [8], based on clam size and density of individuals in the colony. Scattered clam populations (less than 10 individuals/m$^2$) are not considered significant indicators of fluid venting, as clams are able to travel for some distance (note the tracks they leave on the surface of the sediment). Definition of the colony types is as follows:

*Type A*: Large colonies (up to 2 m in diameter), composed of small (5 cm long or less), medium (about 10 cm long) and often large clams (15–25 cm long). Very dense (1000 ind./m$^2$) with strong bioturbation (mud surface is black).

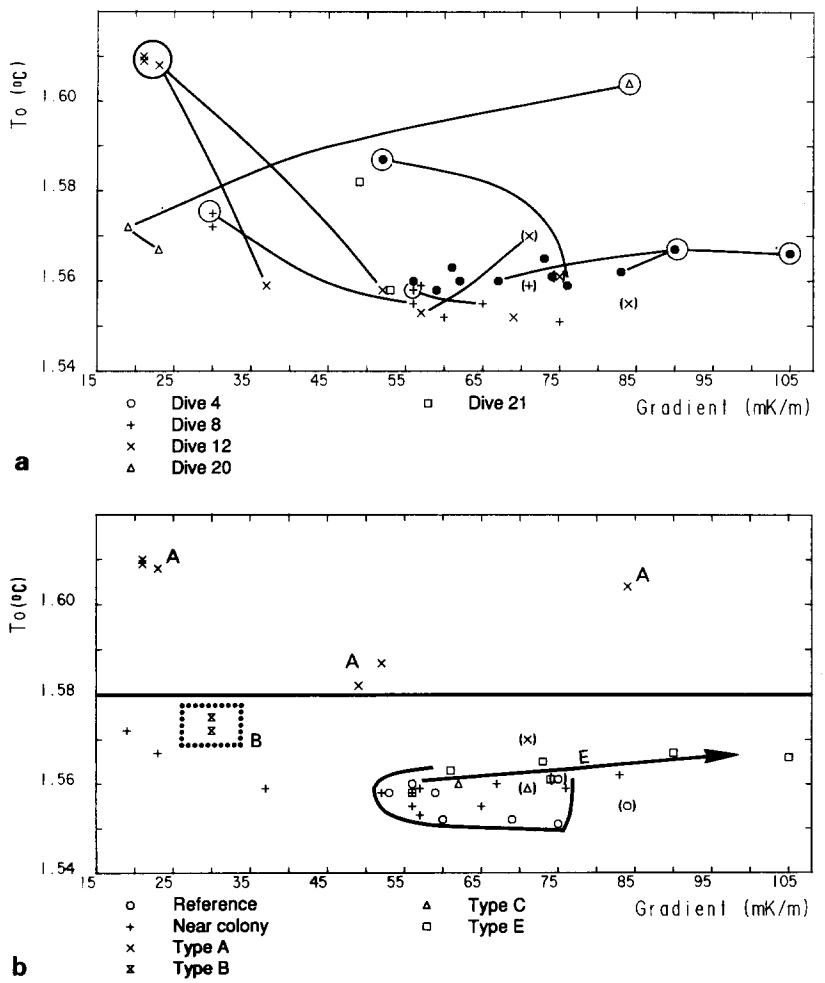


Fig. 2. Plot of extrapolated surface temperature $T_0$ (see section 3.2 for definition) versus average gradient between 20 and 50 cm in the sediment. All the thermal measurements made in zone 1 are plotted, but dubious data are shown in parentheses. (a) Measurements are classified by dive number. Grouped measurements are marked: measurements made inside the clam colony are circled and linked with bold lines to those made in its immediate surroundings (within 2 m). Note that many measurements are isolated. (b) Measurements are classified by site type. Most of the measurements made outside clam colonies cluster around a gradient of 60 mK/m and a $T_0$ of 1.55–1.56°C. Measurements in type E colonies show a continuous trend (symbolized by the arrow) from normal to high gradients; type A colonies have high $T_0$ ($T_0 > 1.58$°C), which is characteristic of high-velocity upward fluid flow; $T_0$ in surveyed type B colonies is slightly lower, at about 1.57°C, and the gradient is very low (30 mK/m).

*Type B*: Small colonies (less than 50 cm diameter) of medium-sized half-buried clams; medium density (50–100 ind./$m^2$).

*Type C*: Colonies composed exclusively of big, half-buried clams at low density (30 ind./$m^2$). These are usually found around "white patches", which are characterized by a very high content of hydrogen sulphide and by $CaCO_3$ saturation [9]. These patches are probably bacterial mats.

*Type E*: Dense colonies of small clams (200 ind./$m^2$). These colonies are usually small (less than 50 cm in diameter). Unlike the other types of colonies, bivalve species in type E colonies are not of the genus *Calyptogena*, but belong to other members of the Vesicomidae family.

### 3.2. Thermal trends

Table 2 lists all the thermal measurements made in the deepest studied area. Thermal gradient values are given by linear regression of the temperature measurements inside the sediment. The bottom-water temperature is not taken into account. The extrapolation of the linear regression to the seafloor ($T_0$) is usually different from the bottom-water temperature (see Table 2). As discussed in section 2.1, the values of $T_0$ computed from measurements made outside clam colonies give a better estimate of the mean temperature at the surface and are used as a reference. For measurements made in active vents, an increase of the extrapolated temperature $T_0$ above this reference results from the curvature of the gradient in the first 20 cm, and is thus indicative of the velocity of fluid flow.

Temperature–depth profiles fall into four different types. Linear profiles are straight lines within the accuracy of measurements. Sublinear gradients have a significant but slight nonlinearity. Their interpretation in terms of water advection is not systematic. The exact boundary between these two is a matter for discussion. The profiles classified as curved have an obvious upward oriented convexity and anomalously high temperatures. They are interpreted as indicative of fluid advection. Finally, profiles categorized as odd have nonlinear z-shaped gradients. Their interpretation is difficult in terms of vertical upward or downward movement of fluid as well as in terms of conductive transient states.

In Table 2, measurements made inside a colony and in its immediate surroundings are grouped (see also Fig. 2a). The distance to the edge of the colony is given but, as this distance was actually measured only during dive 12, it is not usually known accurately. Models presented in the following section indicate that the thermal disturbance fades rapidly away from a colony and that measurements made more than 2 m away should not be perturbed. Measurements made far from colonies (*F* in Table 2) are made at least 10 m from the nearest active site. They were used as references, providing estimates of the background conductive gradient. Those made during dives 4 and 8 (see Fig. 1a) are close enough to the studied colonies to be used for this purpose, but measurement 12-8 (84 mK/m) is too far north and may be biased by variations in the regional gradient. Furthermore, extrapolated surface temperatures indicate that recent variations in bottom-water temperature seem to have been different at the dive 12 reference sites from those near the colony studied during this dive (measurements 12-1 to 12-5).

The background thermal gradient varies between 53 and 75 mK/m in the active area, 60 mK/m being the average value. Outside clams colonies, the extrapolated surface temperature ($T_0$) varies between 1.55 and 1.56°C, depending on the dive and on the location: $T_0$ tends to be slightly higher for measurements made near colonies than for reference measurements. However, both types of measurement define one single dense cluster (see Fig. 2b). Various processes can account for local variations of gradient. We have already discussed the role of the fluctuations of bottom-water temperature. Topograpic disturbance and sediment conductivity variations have also to be considered. However, the plateau on which most of the measurements were made is fairly flat, and is not rough at the scale of the measurements (50 cm). Furthermore, all the measurements were made on flat surfaces where disturbance due to local topography should be small. Larger scale topography seems to have only a small effect, as the gradient does not increase significantly (considering the dispersion of the data) away from the cliff at the southern edge of the plateau. Conductivity measurements on samples from piston cores taken in the Nankai Trough

area vary between 0.7 and 0.85 W $m^{-1}$ $K^{-1}$ [10], but a wider range of variation and higher values are expected if sand layers are present. Carbonate cementation also increases conductivity, but the probe cannot penetrate concretions. All temperature measurements were made in unconsolidated sediments and their conductivity may range from 0.7 to 1.2 W $m^{-1}$ $K^{-1}$ ($\pm 25\%$) if extreme values are considered [7]. Gradient dispersion within the central cluster defined above (Fig. 2b) is actually quite high (almost $\pm$ 20%) and, among other factors, probably results from conductivity variations. Measurements that plot outside this central cluster need another explanation, however.

Conductivity variations may also be responsible for the nonlinearity of thermal profiles. However, reference measurements are quite linear, as exemplified by Fig. 1, and only three of all the measurements made outside clam colonies are classified as "curved" or "odd", and two of those were made at the same station. Thus, we will assume that vertical conductivity variations in the first 50 cm of sediment are not significant.

The two measurements made in white patches associated with type C clam colonies are within this cluster, which suggests that fluid flow there is too low to create significant perturbations. However, more measurements are necessary to make this conclusive.

Type E colonies display a continuous trend from normal to high gradients (100 mK/m), with a comparatively small increase in $T_0$. This is what is expected if colonies are fed by fluids coming slowly from depth (velocity of the order of 10 m/a).

Type A colonies are characterized by a high $T_0$ ($> 1.58$°C) for measurements made inside the colony, which is indicative of very high Darcian flow velocities (of the order of 100 m/a). However, gradients between the depths of 20 and 50 cm can be much lower than normal in these type of colonies, which suggests convection, as will be discussed later. An additional feature is the occurrence of very low gradients near two of these colonies (with $T_0$ close to reference temperature), which we attribute to downwelling of seawater.

The two type B colonies investigated have a low temperature gradient (30 mK/m), and a relatively high $T_0$, suggesting that they are similar to type A colonies but with weaker flow. Measurements made near these colonies are normal, suggesting that if convection is occurring, it may be limited to the colony itself.

In the following part we will concentrate on the study of one colony each of types A, B and E. In each case, several measurements were made within and outside the colony. Convection will at first not be considered, as the observed low gradients inside type A and B colonies can also be explained if fluids flow horizontally into the conduit that feeds the colony.

## 4. Modeling of fluid advection

In order to reproduce the different thermal characteristics of the different colony types, we used models of the same type but with different geometries of fluid flow. However, all the models are symmetrical along a vertical axis and the diameter of the porous permeable conduit which feeds the colony is taken as equal to 60 cm, but the length of the conduit varies. Fluid flow is forced by a fixed pressure difference between the upper (the seafloor) and lower boundaries of the model (advection as opposed to convection). The assumed permeability structure controls the geometry of fluid flow. The density of fluid is assumed to be constant, and equal to the density of seawater. Convection is thus impossible and all fluid expelled through the colony comes through the base of the mesh. Excess pore pressure and fluid flow velocity fields are first computed from the boundary conditions, assuming no water storage (and thus are steady-state), with no sources within the mesh. Then the convection–diffusion equation is solved for the temperature field, using the fluid flows previously calculated. The temperature can be computed in steady-state or transient state. The initial state is then the steady-state without fluid flow, and fluid flow is taken constant throughout the computations. In short, water flow and thermal problems are solved sequentially and both equations are purely linear.

The physical parameters used are given in Table 1. The most sensitive parameter is the thermal conductivity of sediment, which is assumed to be $\Lambda = 1$ W $m^{-1}$ $K^{-1}$. For a given geometry, the steady-state temperature field does not change if the ratio $V_D/D$ of the Darcy veloc-

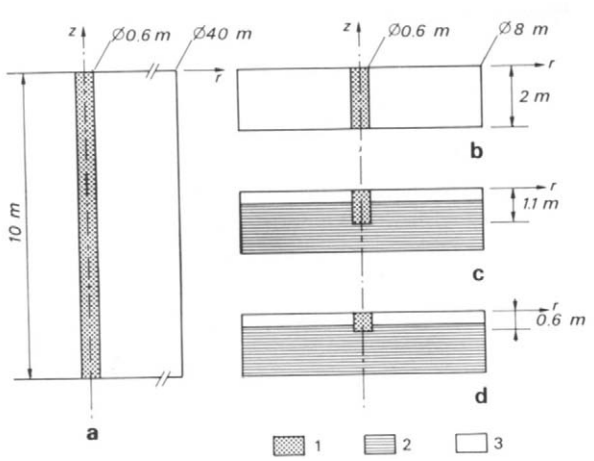


Fig. 3. Geometry and permeability structure of the various models of clam colonies. *1* = conduit ($k = 10^{-10}$ m$^2$); *2* = layered turbiditic sediment (horizontal permeability $k_{rr} = 10^{-11}$ m$^2$ and vertical permeability $k_{zz} = 10^{-13}$ m$^2$); *3* = homogeneous mud ($k = 10^{-13}$ m$^2$). (a) Model with a long cylindrical conduit of 10 m in length. (b) Model with a short cylindrical 2 m conduit. (c and d) Short conduit models with conduit ending inside the mesh; the high horizontal permeability outside the conduit allows lateral fluid recharge.

ity over the thermal diffusivity remains constant.

The geometry and the velocity of fluid flow are adjusted for the model to fit the temperature data. But pressure gradient and permeabilities are not known, and cannot be constrained by this method. The permeability and pressure gradient values given here are only indicative, and based on the assumption that the pressure gradient is very close to hydrostatic, which is consistent with the results of the "puppi" (pop up pore pressure instrument) experiment [11]. However this experiment was not very conclusive, and one may assume pore pressure gradients up to two orders of magnitude higher than those used for this modeling. The fluid flow would however be the same if at the same time permeability is lowered by two orders of magnitude.

### *4.1. Long conduits*

The first finite element model is a vertical conduit of radius 30 cm and of length 10 m (see Figs. 3a and 4). The purpose of this model being to approximate the solution for an infinitely long conduit, the choice of the conduit length is arbitrary, provided it is much larger than the conduit diameter. The boundary conditions are a fixed hydraulic head and temperature at the surface and at a depth of 10 m. The condition on the lateral boundary is no water flow and no heat flow. This boundary is set at a distance of 20 m from the centre so that the perturbation induced is small.

As upflowing fluids loose much more heat through the walls, the temperature profile with depth in a long cylindrical conduit is significantly different from that obtained with one-dimensional models or two-dimensional models with a

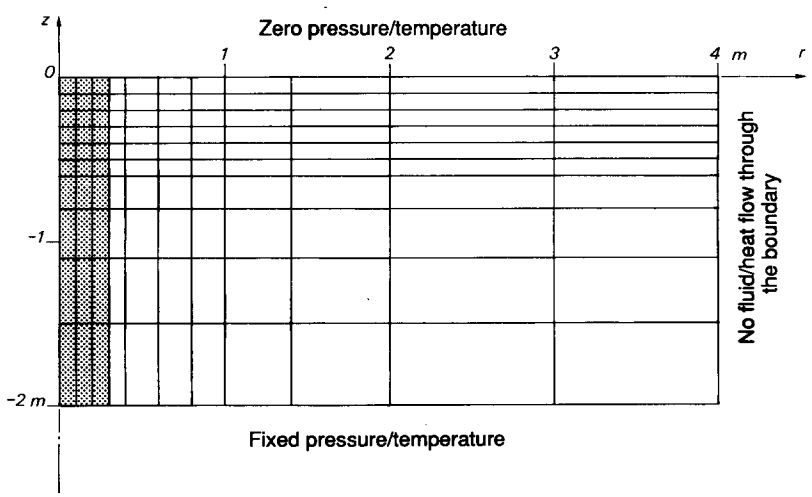


Fig. 4. Finite element mesh and boundary conditions used for advection models with conduits that are 2 m in length or shorter. For the 10 m long conduit, elements with 1 m node spacing are added at the bottom and at the outer boundary.

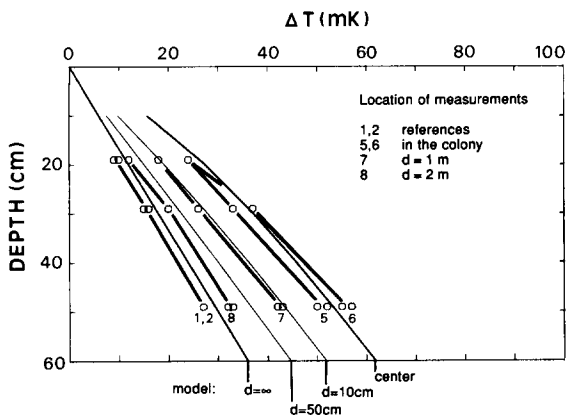


Fig. 5. Temperature measurements and model in a type E colony (dive 4); $d$ is distance from the edge of the colony. Darcian flow velocity is 30 m/a.

planar conduit [5]. In particular, gradient does not always tend to zero with depth, even for high flow rates (mathematically, $zU_D/D \gg 1$ does not imply $\partial T/\partial z \approx 0$). Consequently, the long cylindrical conduit model is not appropriate for colonies having a low thermal gradient.

The permeability inside the conduit is taken as equal to $10^{-10}$ m$^2$, corresponding to a clayless coarse sand [12], and is 1000 times higher than in the surrounding sediment. Because the Darcian flow velocity inside the conduit is typically of a few tens of metres per year, the Darcian flow outside is between 1 and 10 cm/a, which only increases the thermal gradient by a few percent if the lower boundary condition is set at 10 m. The corresponding curvature of the temperature profile is undetectable by temperature measurements in the first 50 cm below the surface.

The steady-state temperature profiles inside the conduit for an excess pore pressure gradient of 10 Pa m$^{-1}$, and thus a Darcy velocity of 30 m/a, fit well the data from a type E colony (see Fig. 5). However the decrease in the thermal gradient away from the conduit occurs more rapidly for the model: measurement 4-7, made about 1 m away from the rim of the conduit is fit by a model profile obtained just 10 cm away from the conduit. This may indicate that fluid advection does not occur only in the colony but that it is at a maximum there.

### 4.2. *Short conduits*

Most other colonies have temperature–depth profiles implying that the temperature of fluids in the conduit equilibrates with the background gradient at a shallow depth. This is especially noticeable for the type B colonies studied during dive 8. The temperatures measured at the 50 cm depth are roughly the same within and outside the two type B colonies (see Fig. 6). For the type A colony studied during dive 12, as the temperature elevation above reference is 60 mK both at the 30 and 50 cm depths, the fluid temperature is then expected to equilibrate with the background at about the 1 m depth (see Fig. 7). As no significant fluid source can exist at such shallow depths, a mechanism is required to explain this phenomenon.

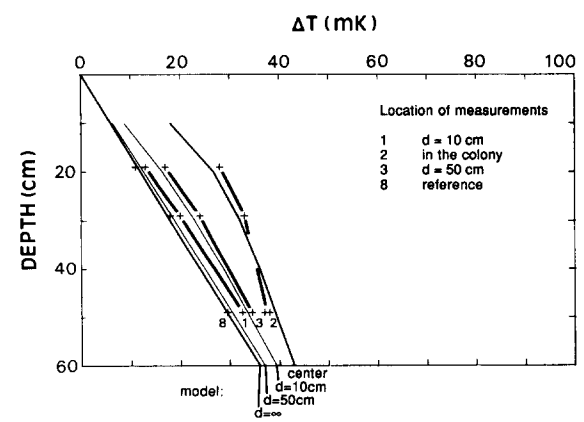


Fig. 6. Temperature measurements and model in a type B colony (dive 8); $d$ is distance from the edge of the colony. Darcian flow velocity is 70 m/a.

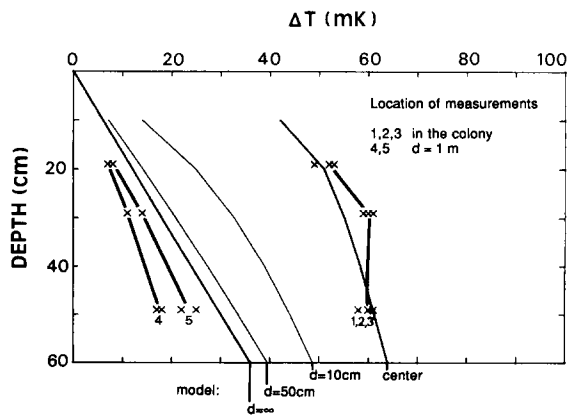


Fig. 7. Temperature measurements and model in a type A colony (dive 12); $d$ is distance from the edge of the colony. Darcian flow velocity is 150 m/a.

Permeability in the conduit is again taken equal to $10^{-10}$ m$^2$, but the conduit now ends inside the finite element mesh, the lower boundary being at a depth of 2 m (see Figs. 3 and 4). Outside the colony, the sediment from the surface to 40 cm deep is assumed to be homogenous sandy mud and to have a permeability of $10^{-13}$ m$^2$, which is the same as for sediment surrounding the conduit in the long conduit model. We assume that, below this surface layer, the sediment consists of turbidites in which fluid can flow along subhorizontal sandy layers, whereas clayey or silty layers prevent fluid from escaping upward. Permeability within this turbiditic domain is assumed to be uniform, but anisotropic, which is easier to handle with finite elements than discrete thin strata. As two orders of magnitude of stratigraphic anisotropy is reasonable for turbiditic sediment [13], horizontal permeability is taken equal to $10^{-11}$ m$^2$ and vertical permeability equal to $10^{-13}$ m$^2$.

Below the end of the high-permeability conduit, fluid slowly and uniformly seeps upward. Between the base of the conduit and the 40 cm depth, most of the fluid converges towards the conduit. The remaining fluid seeps through the isotropic surface layer. In this model, there is significant fluid advection outside the conduit, of the order of 10 cm–1 m/a (Darcy velocity). Note that the total amount of fluid collected in the central conduit is largely dependent on the radius of the outer boundary. In our model, fluid is drained from a 4 m radius area. An actual colony may drain a larger area if it is isolated and if permeable layers extend beyond without discontinuity.

Actually, fluid may not seep uniformly and vertically at depth. For example, flow may also be channeled by fractures, joints or sand dykes. One can also envisage that fluid migrates along sand layers for long horizontal distances before reaching the colony. These two cases would require truly three-dimensional modeling, but they do share with the present model its main feature: the conduit that feeds the colony is not deeply rooted and fluids have to converge on the colony along shallow permeable layers.

The results for the steady-state are compared with the data in Figs. 6 and 7. A consequence of the vertical fluid flow outside the colonies is an increase of about 5% of the background gradient in the first 50 centimetres (the lower boundary being at 2 m). It follows that part of the measured background conductive gradient may be due to residual flow. In Figs. 6 and 7, only corrected profiles are given.

It appears that the measured temperature elevation in the conduit can be simulated with a 60 cm long conduit (and a Darcian flow velocity inside the conduit of 70 m/a) for type B colonies, and with a 110 cm conduit for the dive 12 type A colony (and a Darcian flow velocity inside the conduit of 150 m/a). However, the bend in the measured profiles at around the 30 cm depth is not obtained with any reasonable parameter set (the calculated profiles tend to be almost linear). This is especially true for the type A colony, where the measured temperatures at the 30 and 50 cm depths are identical, but this feature could be transient. The OT 6000 long-term thermal observatory recorded temperature fluctuations of $\pm 0.05$°C at a depth of 34 cm within the sediment in another active type A colony. Foucher et al. [7] interpret these fluctuations as being due to variations in flow rate. Thus, it can be expected that the temperature data from dive 12 also correspond to a transient state. However, the fluctuations recorded by the OT 6000 represent less than $\pm 10\%$ of the temperature difference between the seafloor and the 34 cm deep probe. Consequently, we assume that the flow velocity can still be roughly estimated from a steady-state model.

### *4.3. Extension of results to other colonies*

These three models and an additional one featuring a conduit of 2 m in length are compared with all other exploitable data sets and the velocity of fluid flow is adjusted for each case. The best fitting parameters are given in Table 3, where they are compared with the Darcian flow velocities estimated with the one-dimensional model.

## 5. Convection models

### *5.1. Arguments in favour of convection*

A first argument comes from the measurement of very low gradients around two type A colonies. Measurements 12-4 and 12-5 were taken on each

side of a type A colony, 1 m away from the rim (see Fig. 7). One gave a low value (37 mK/m), while the other (52 mK/m) is compatible with other measurements of background gradients, which excludes the possibility that the low gradient is characteristic of the site. Considering the ratio of these two values (1.4) it is possible, but unlikely, that a conductivity variation can account for the difference in gradient. There is no significant elevation of the extrapolated surface temperature, and therefore this measurement cannot be interpreted as the consequence of upward fluid flow. Local downwelling of fluid is, in contrast, a likely interpretation. An even lower gradient value (20 mK/m) was obtained 1.5 m off an active type A colony (dive 20), near a cluster of dead clam shells. This indicates past (but recent) activity. Such a low value cannot be the consequence of locally higher conductivity. This measurement is somewhat confusing because there is an upward convexity of the temperature profile and the extrapolated surface temperature is slightly increased. (However, the reference surface temperature is not known accurately for this dive.) But it is equally difficult to interpret this measurement simply in terms of upward flow or by a recent change in bottom-water temperature. Downflow is again the most likely interpretation.

One measurement made only 10 cm away from the edge of a type B colony (8-1) was normal both in terms of gradient and of extrapolated surface temperature (see Fig. 6). This is not what is predicted by the advection model and suggests that the rim of the colony is cooled by downflow in the conduit itself. Small-scale convection below the colony has the advantage of providing an easy way to explain the uniformity of temperatures measured at the 50 cm depth inside and outside type B colonies. On the other hand, the surprising uniformity of the three thermal measurements (12-1,2,3; see Fig. 6) made at three different locations in a single type A colony implies that fluid flow is fairly uniform within the colony and that downflow occurs elsewhere. The convection has then to occur on a larger scale. Conforming the results of advection models, the base of the convection cell should be at a depth of 1 or 2 m, and low gradient measurements would indicate that downflow occurs 1 or 2 m away from the colony, and possibly further away than this.

An other argument is indirect and based on the fact that the total fluid flux in the area deduced from flow values in the colonies (about 200 $m^3/a$ per metre of subduction zone, see section 6) is too high to be compatible with the measured 60 mK/m background thermal gradient. This point is discussed in more detail by Le Pichon et al. [14], according to whose estimates the total heat flux (advective and conductive) through colonies is much smaller than the background conductive flux outside the colonies integrated over the active area. Thus, the total heat flux through the active area can be approximated. The amount of water coming from depth is then estimated using simple thermal models. The values obtained imply dilution with seawater by a factor of 6 to 30, depending on the temperature gradient assumed for thermal equilibrium in the absence of fluid flow (40–60 mK/m) and on the depth at which mixing is assumed to occur (1–20 m).

### *5.2. Is convection driven by temperature or salinity?*

Free convection has to be driven by an inverted density gradient, which can be caused either by the thermal gradient or by a salinity difference between seawater and seeping fluids. Equations governing convection in a porous medium can be written in the same way for both cases. For the thermal problem, the Rayleigh number is:

$$Ra_t = \frac{\rho g \cdot \alpha_t \Delta T \cdot Hk}{\mu D_t} \tag{3}$$

$\rho g$ is the hydrostatic pressure gradient: $10^4$ Pa $m^{-1}$
$\alpha_t$ is the coefficient of thermal expansion of water: $10^{-4}$ $K^{-1}$ under 400 bars at 2.5°C
$\Delta T$ is the temperature difference between lower and upper boundaries: $\Delta T/H = 60$ mK/m
$H$ is the characteristic size of the system
$\mu$ is the viscosity of water, around $10^{-3}$ Pa s
$D_t$ is the thermal diffusivity $\Lambda/(\rho c)_w$, $2.5 \times 10^{-7}$ $m^2/s$ if dispersivity is not taken into account
The chemical Rayleigh number is:

$$Ra_c = \frac{\rho g \cdot \alpha_c \Delta S \cdot Hk}{\mu D_c} \tag{4}$$

$\alpha_c$ is the coefficient relating salinity and density variations at a given temperature:

$$\alpha_c = \frac{1}{\rho}\left(\frac{\partial \rho}{\partial S}\right) \quad (5)$$

$\alpha_c = 0.77$ at 0°C [12].

$D_c$ is the diffusivity of the solute, $D_c = d_0 + \beta |U_D|$; $d_0$, the molecular diffusivity, is of the order of $10^{-9}$ m$^2$/s; $\beta$, the coefficient of dispersivity, is very dependent on the scale of the system and on its heterogeneity [12]. For a problem on the scale of a few metres, $\beta$ is probably between 1 and 10 cm. Consequently, $D_c$ is between $10^{-9}$ m$^2$/s and $3 \times 10^{-7}$ m$^2$/s (with $U_D <$ 100 m a$^{-1}$).

$\Delta S$ is the salinity difference between the upper and lower boundaries. The salinity of seawater is 34‰. Chlorinity of interstitial pore water sampled in white patches is about 0.95 times that of seawater samples, indicating that the salinity of the undiluted fluid source is at least 1.7‰ (3.4 × 0.05) less than that of seawater [9]. In the Barbados area, fluids sampled in a mud volcano situated seaward of the deformation front are half as saline as seawater [3]. At the ODP Leg 110 site, fluids flowing along the décollement and along out-of-sequence thusts drilled on an inner portion of the wedge are both 10–30% less saline than seawater, although the fluids are of a different origin for each case [15]. Recent drilling through the toe of the Nankai wedge (ODP Leg 131) showed a drop in chlorine concentration associated with the hemipelagic section that was attributed to past fluid injection [16]. These showed that an original fluid source of low salinity is very likely in the context of an accretionary complex and that the salinity difference expected is more than 0.1‰ but less than 17‰. The source of low-salinity water is unclear (see [14], for example).

The critical Rayleigh number is about 40 for closed roll convection in a permeable horizontal stratum with fixed temperatures, or salinity, at the boundaries [17]. If the fluid is allowed to flow freely through the upper boundary the critical Rayleigh number is smaller, of the order of ten.

Then, for the thermal problem, $Ra = 10$ implies $H^2 k = 3.33 \times 10^{-8}$ m$^3$. If we suppose that

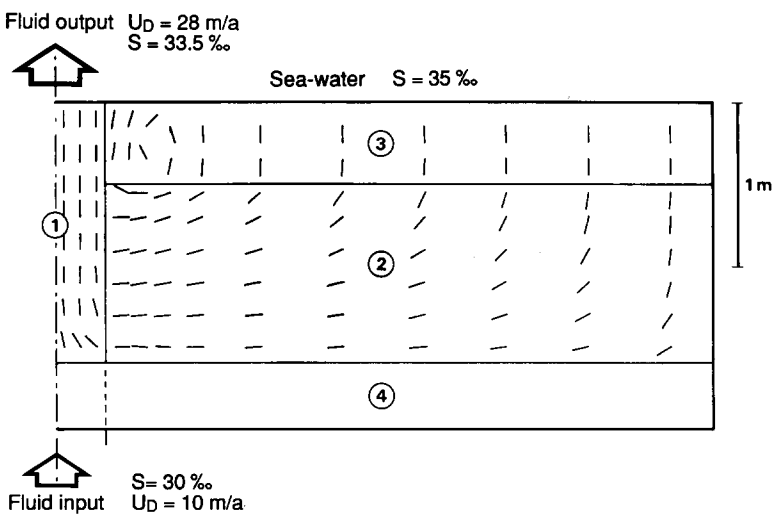


Fig. 8. Finite element model of small-scale (2 m) haline convection around a high-permeability conduit. Boundary conditions for the flow equation are zero pressure on upper boundary, fixed flow below the base of the conduit ($U_D = 10$ m/a) and no flow elsewhere. Boundary conditions for the salt transport equation are fixed salinity on the upper boundary (35‰) and below the base of the conduit (30‰) and no flow elsewhere. The salinity difference between fluid source and seawater is only 5‰. Upcoming fluids are diluted with seawater by a factor 3.4 in the convection cell. Dashes show direction of fluid flow but have a constant length. Permeabilities are as follows: (*1*) $k = 10^{-10}$ m$^2$; (*2*) $k_{rr} = 2 \times 10^{-11}$ m$^2$ and $k_{zz} = 2 \times 10^{-12}$ m$^2$; (*3*) $k = 2 \times 10^{-12}$ m$^2$; (*4*) $k = 10^{-12}$ m$^2$. Layer (*4*) is used to isolate the lower boundary condition ($S = 30$‰ below the conduit, no mass flow elsewhere) from the convection cell. If this is not done, a lot of salt leaves the finite element mesh by diffusion through the lower boundary of the conduit, which modifies the results.

convection occurs between the seafloor and the 2 m depth, $k$ must be higher than $0.8\ 10^{-8}$ m$^2$, which is about the permeability of stacked pebbles. If a permeability of $10^{-10}$ m$^2$ is assumed, $H$ should be 20 m or more.

For the chemical problem, $Ra = 10$ implies $10^{-13} < Hk < 4 \times 10^{-10}$ m$^3$, depending on the values chosen for $D_t$ and $\Delta S$. Salinity-driven convection at the 1 m scale thus appears to be compatible with a high conduit permeability ($10^{-10}$ m$^2$ or less).

Because of the complex geometry of the system and of its highly heterogenous permeabilities, one cannot rely uniquely on the computation of a Rayleigh number as a criterium for convection. However, thermal convection can be ruled out on this basis.

*5.3. Modeling of chemical convection*

A finite element model has then been used to check that convection is actually possible with a salinity difference of only a few permil (Fig. 8). The permeability structure of the model is also given in this figure, and is very similar to that of the short conduit model. Fluid of constant salinity is injected at the base of the high-permeability conduit ($k = 10^{-10}$ m$^2$) and as its density is lower than that of the pore water in the surrounding sediments, seawater flows into the conduit from the sides and mixes with the low-salinity fluid. In the case shown in Fig. 8 the difference in salinity is 5‰ between seawater and the injected fluid, and the input flow is 2.8 m$^3$/a, which corresponds to a velocity of 10 m/a in the conduit (conduit radius is 0.3 m). The model predicts that 5.2 m$^3$ of seawater per year would flow into the conduit from the sides along strata of higher permeability ($k_{rr} = 2 \times 10^{-11}$ m$^2$) and the flux through the seafloor of mixed fluids is 8 m$^3$/a, corresponding to an average velocity of 28 m/a in the conduit. The dilution factor here is 2.85, which is lower than the factor of 6 to 30 estimated from the heat balance of the active area [14]. In this model, fluid downflow is very slow (maximum 10 cm/a) as it has to cross low-permeability layers and spreads out over a large area (model radius is 4 m), and it is not sufficient to explain the observed reduction in gradient. Fluid downwelling may in the real world be localized in high-permeability conduits, as is upwelling, but this feature cannot be modeled with two-dimensional finite elements. Modeling also showed that if the horizontal permeability is suppressed, convection may still occur but is confined inside the high-permeability conduit. Salinity, flux of incoming fluid and permeability of the conduit are the parameters that control the velocity of fluid venting, almost independently of the permeability around the conduit.

As convection implies that fluid flows into the conduit, the pore pressure inside the conduit is lower than the pore pressure outside the conduit at the same depth. Furthermore, as downflow is supposed to occur somewhere outside the colony, the pore pressure gradient there is necessarily smaller than the hydrostatic gradient in seawater. Thus, for a given density of diluted fluid flowing in the conduit, the maximum Darcian flow velocity ($U_{\mathrm{Dmax}}$) compatible with salinity-driven convection can easily be estimated:

$$U_{\mathrm{Dmax}} = \frac{kg}{\mu}(\rho_{\mathrm{seawater}} - \rho_{\mathrm{mixed\ fluids}}) \qquad (6)$$

where $k$ is the permeability in the conduit, $\mu$ is the viscosity of water ($10^{-3}$ Pa s), $g$ is gravity (10 m s$^{-2}$), and $\rho$ is density. If $k$ is assumed to be equal to $10^{-10}$ m$^2$, which can be considered as an upper bound, a Darcian flow velocity of 100 m/a can be obtained in the conduit if $\Delta\rho = 3$ kg/m$^3$, which corresponds to a salinity difference of 4.5‰ between seawater and the diluted fluids in the conduit. Note that in the finite element model shown in Fig. 8, $U_{\mathrm{D}}$ in the conduit (average 28 m/a) is close to the maximum value given by eq. (6) ($U_{\mathrm{Dmax}} = 32$ m/a for $\Delta S = 1.5$‰).

The dilution factor cannot be estimated as the original salinity of the migrating fluid is not known. However, it cannot be more than 10 for reasonable values of permeability (less than $10^{-10}$ m$^2$), and flow rates of more than 10 or 20 m/a cannot be driven by salinity contrast if conduit permeability is less than $10^{-11}$ m$^2$.

## 6. Total flux through clam colonies at site 1

One dive was devoted to a statistical estimate of the density of clam colonies and of the area of seafloor covered by clam colonies (dive 23, scientific observer (Sci. Obs.) M. Sibuet). The sub-

mersible followed straight parallel lines 100 m apart, evenly exploring a zone of 625 m in length and 500 m in width along the upper part of the slope and on the plateau. Images recorded by a CCD camera carried on the submersible were used as a reference for counting colonies of different types and estimating their surface area [7,8]. The width of the camera field happened to be not significantly different from the altitude of the submersible itself, which is continuously measured by a pinger. The mean value of the field width is thus about 2.3 m for dive 23. Consequently, the area actually seen on the video during dive 23 represents 4% of the studied zone (see Table 4).

The distribution of type A colonies in the zone is highly inhomogenous: two-thirds of the counted colonies are found in a small 10,000 $m^2$ area, in which the second site of deployment of the OT 6000 and "Puppi" measurement 6 are also located. This zone was explored, during dive 23, more intensively than the rest of the surveyed area as the divers were looking for a convenient site to conduct a biological experiment. We estimate that 7.5% of the surface of this colony cluster has been explored.

Other colony types appear to have a more homogeneous distribution. Thus, we simply multiply the observed colony surface by 25 to estimate the total area covered by type B, type C and type E colonies.

Dives 12 (Sci. Obs. P. Schultheiss) and 17 (Sci. Obs. N. Chamot-Rooke) extended as far as 1.5 km from the surveyed area, and found venting sites as well: a big cluster of type A colonies (dive 17) and spread-out type C colonies in small erosional gullies (dive 12). Dive 3 (Sci. Obs. Z. Takeuchi) climbed the slope east of the surveyed area and found some biological activity. Further north, on top of the plateau, two clusters of type A colonies were found during dive 21 (Sci. Obs. G. Furuta). This showed that, whereas large sec-

TABLE 4

Total fluid flux in zone 1

| | |
|---|---|
| Zone 1 is a box 500 m x 625 m (500 m orthogonal and 625 m parallel to deformation front) | |
| Average width of image on CCD | 2.3 m |
| Distance covered during dive 23 | 5,370 m |
| Surface explored during dive 23 | 12,300 $m^2$ = 4 % of Zone 1 |
| Main cluster of colonies | 10,000 $m^2$ |
| Explored surface in main cluster | 750 $m^2$ = 7.5 % of cluster area |

| Colony Type | Nb | Surface | | nominal fluid flow | total flux | mean flux [c] |
|---|---|---|---|---|---|---|
| | | $m^2$ | % [a] | m/a | $10^3$ $m^3$/a | $m^2$/a |
| A | 122 | 60 | 0.5 | 100 | (150) | (240) |
| A: Cluster | | 40 | 5. [b] | 100 | 53 | 85 |
| A: Background | | 20 | 0.16 | 100 | 50 | 80 |
| A: Total | | | | | 103 | 165 |
| B | 31 | 7.8 | 0.06 | 70 | 14 | 22 |
| C | 18 | 1.9 | 0.015 | 0? | 0? | 0? |
| E | 274 | 25 | 0.2 | 10 | 6.2 | 10 |
| Total | 445 | 94 | 0.76 | - | 123 | 197 |

[a] Surface of observed colonies in percent of the total explored area

[b] Surface of observed colonies in percent of the area explored in the main cluster

[c] Mean fluid flux is in cubic metres per year per metre width of subduction zone

tors of the 500 m wide active zone are empty of clams, other clusters of colonies could be found in either direction along the anticline.

Results of the colony count are given in Table 4. The total fluid flux out of the colonies was then estimated using a nominal value of Darcian flow velocity for each type of colony. The total amount of fluid expelled is huge, of the order of 200 $m^3$ $a^{-1}$ per metre of subduction zone ($m^2$ $a^{-1}$). Most of the fluid are expelled through type A colonies both because they cover more surface than other types of colonies and because they are more active. But as convection is suspected to occur in association with this type of colony, the fluid flux actually coming from depth is not known accurately. The maximum value of deep fluid flux compatible with the value of background heat flow is discussed in Le Pichon et al. [14] and is compatible with dilution by subsurface convection by a factor of 6 to 10.

## 7. Conclusion

The velocity of upward fluid flow, and the flow pattern, appear to be correlated with the intensity and type of biological activity. Slow seepage ($< 10$ m/a) of hydrogen-sulphide rich fluid favours the development of white bacterial mats. Colonies of large *Calyptogena* sp. (type C) are occasionally found around these white patches. Rapid flow of diluted fluid (100 m/a) is characteristic of the densest colonies of *Calyptogena* (type A). Another characteristic of type A colonies is the very shallow depth (1 or 2 m) of the fluid source inferred from thermal modeling. We propose that mixing with seawater downwelled outside the colony is cooling the upcoming fluid. Type B colonies are not markedly different but smaller and less dense. Their recharge depth is even shallower, suggesting downflow of seawater in the conduit itself. Small bivalves from the Vesicomidae family tend to gather in small clusters which may be found in great number over large surface areas (type E). Fluid flow velocity in these vents is quite variable but always smaller than in type A or B colonies. When fluid flow determination is possible ($U_D > 10$ m/a) temperature measurements also indicate that the fluid conduit is continuous at depth and that mixing with seawater may only occur at a depth of more than 10 m. Thus, these bivalves are probably more efficient than *Calyptogena* sp. in the exploitation of pervasive flow and/or of low flux conduits. Note that these characteristics of the vents preclude determining the upwelling temperature at great depths before mixing occurs.

A statistical study of the surface covered by each type of colony indicates that most of the fluid is vented through type A colonies [7]. The total estimated fluid flux is about 200 $m^2$ $a^{-1}$. This value is more than one order of magnitude larger than that expected to come from steady-state compaction of the wedge [14]. The absence of a significant increase in the background heat flow in the area of venting indicates that the fluid flux actually coming from depth is more probably of the order of a few tens of square metres per year [14].

Type A colonies are almost exclusively found on the summit plateau, while white patches and type C colonies are only found on the upper slope along the probable outcrop of a flat thrust or shallow décollement, situated 20 m below the top of the anticline [18]. This enables us to propose the following scheme for fluid flow: A flux of 20–40 $m^2$ $a^{-1}$ of fluid having a high sulphide content and a low salinity flows along a flat thrust connected to the décollement by the second major active thrust in the area. The salinity contrast between the incoming fluid and seawater can cause convection to occur at two different scales: between the décollement and the surface, and near the surface around the vents. Thermal arguments led to the conclusion that some amount of dilution is likely to occur at the level of the flat thrust [14]. Type E colonies, which are found all over the active zone, possibly vent fluids already diluted at depth. Wherever fluid of deep origin reaches the seafloor on the plateau sufficiently undiluted, a small-scale convection cell would form, associated with a type A or type B colony. Note, however, that models indicate that such a mechanism for convection would require that the permeability of the sediment is locally as high as $10^{-11}$ or $10^{-10}$ $m^2$ below the convecting colonies, and we do not know if this is true. A fraction of the original fluid continues to flow slowly along channels in the shallow décollement zone, and possibly along strata, and feed chimneys, bacte-

rial mats and type C colonies that are found exclusively along the flat thrust outcrop.

## Acknowledgements

F. Harmegnies from Ifremer (Brest) built and operated the thermal instrument. P. Henry did most of the thermal modeling at the University of California at Berkeley in the laboratory of C. Wang, using FEAP, a finite element program developed by R. Taylor. We also thank P. Goblet from the *Ecole des Mines de Paris* at Fontainebleau who helped us in using his METIS finite element program for modeling of convection.

We thank three anonymous reviewers for their careful reviews.

## References

1 E. Suess, B. Carson, S. Ritger, J.C. Moore, M.L. Jones, L.D. Kulm and G.R. Cochrane, Biological communities at vent sites along the subduction zone off Oregon, in: The Hydrothermal Vents of the Eastern Pacific: An Overview, Biol. Soc. Wash. Bull. 6, 474–484, 1985.

2 X. Le Pichon, T. Iiyama, J. Boulègue et al., Nankai Trough and Zenisu Ridge: A deep-sea submersible survey, Earth Planet. Sci. Lett. 83, 285–299, 1987.

3 X. Le Pichon, J.-P. Foucher, J. Boulègue, P. Henry, S. Lallemant, M. Benedetti, F. Avedik and A. Mariotti, Mud volcano field seaward of the Barbados accretionary complex: a submersible survey, J. Geophys. Res. 95, 8931–8944, 1990.

4 J.C. Faugères, E. Gonthier, R. Griboulard, D. Jollivet and G. Vernette, Morphology, microphysiography and sedimentary and biology patterns of surficial deposits in the South Barbados prism: Record of recent and present active tectonics, Proc. ODP, Sci. Results 110, 111–126, 1990.

5 P. Henry, S.J. Lallemant, X. Le Pichon and S.E. Lallemand, Fluid venting along Japanese trenches, tectonic context and thermal modeling, Tectonophysics 160, 277–292, 1989.

6 B. Carson, E. Suess and J.C. Strasser, Fluid flow and mass flux determinations at vent sites on the Cascadia margin accretionary prism, J. Geophys. Res. 95, 8891–8897, 1990.

7 J.-P. Foucher, P. Henry et al., Time-variations of fluid expulsion velocities at the toe of the eastern Nankai accretionary complex, Earth Planet. Sci. Lett., this issue.

8 M. Sibuet, A. Fiala, J.P. Foucher and S. Ohta, Spatial distribution of clam colonies at the toe of the Nankai accretionary prism near 138°E, Int. Conf. Fluids in Subduction Zones, Paris, 1990 (Abstr.).

9 J. Boulègue, L. Aquilina, A. Mariotti, T. Gamo and H. Sakai, Chemistry of fluids in the Kaiko-Nankai area (Nankai accretionary prism), Int. Conf. Fluids in Subduction Zones, Paris, 1990 (Abstr.).

10 M. Kinoshita and Y. Kazumi, Heat flow: Basic data, In: Preliminary Report of Hakuo-Maru Cruise KH 86–5 (ODP Site Survey), A. Taira, ed., pp. 51–67, ORI, Tokyo, 1988.

11 X. Le Pichon, K. Kobayashi and Kaiko-Nankai Scientific Crew, Fluid venting activity within the eastern Nankai Trough accretionary wedge: a summary of the 1989 Kaiko-Nankai results, Earth Planet. Sci. Lett., this issue.

12 G. de Marsily, Hydrogéologie Quantitative, 215 pp., Masson, Colloq. Sci. Terre, Paris, 1981.

13 F.L. Horath, Permeability variation in the Cascadian accretionary prism: examples from the Oregon prism and Olympic peninsula melanges, M.S. Thesis, Univ. California, Santa Cruz, 1989.

14 X. Le Pichon, P. Henry and the Kaiko-Nankai Scientific Crew, Water budgets in accretionary wedges: A comparison, Philos. Trans. R. Soc. London A335, 315–330, 1991.

15 J.C. Moore, A. Mascle et al., Tectonics and hydrogeology of the northern Barbados Ridge: results from Ocean Drilling Program Leg 110, Geol. Soc. Am. Bull. 100, 1578–1593, 1988.

16 M. Kastner, T. Gamo, J.M. Gieskes and Leg 131 Shipboard Scientists, Hydrogeochemistry of the Central Nankai Trough: Evidence for past or present fluid flow, Int. Conf. Fluids in Subduction Zones, Paris, 1990 (Abstr.).

17 M. Rabinowicz, J.-L. Dandurand, M. Jakubowski, J. Schott and J.-P. Cassan, Convection in a North Sea oil reservoir: Inferences on diagenesis and hydrocarbon migration, Earth. Planet. Sci. Lett. 74, 387–404, 1985.

18 N. Chamot-Rooke, S.J. Lallemant, X. Le Pichon et al., Tectonic context of fluid venting at the toe of the eastern Nankai accretionary prism: Evidence for a shallow detachment fault, Earth Planet. Sci. Lett., this issue.